



Investigation of Electrical Parameters of Amorphous–Crystalline Silicon Heterojunction Solar Cell: Correlations Between Carrier Dynamics and S-Shape of Current Density–Voltage Curve

Sapna Mudgal , Sonpal Singh, and Vamsi Krishna Komarala 

Abstract—We have analyzed a-Si:H(p)/a-Si:H(i)/c-Si(n) heterojunction silicon solar cell having the S-shaped current density–voltage characteristics with a low fill factor and open-circuit voltage, using quantum efficiency (QE) characterization technique under forward/reverse voltage and different light (blue, infrared, and white) bias conditions. The curvature of S-shape is sensitive to excitation light intensities because of modification in junction barrier potential (variation in quasi-Fermi levels splitting). With forward-bias voltage alone near/above S-shaped region, cell's QE is uniformly reduced because of reduction in junction field and dominance of barrier for collection of holes. However, with blue and white light at bias voltages close to S-shaped characteristics, a uniform improvement of QE in broad wavelength region is observed because of defects saturation at the junction interface and photoconductivity in the a-Si layers. With white light and voltage bias, cell's QE is anomalously improved and it has even crossed the QE response at no voltage/light bias conditions in the blue region because of defects saturation in a-Si:H layers, whereas under infrared light and voltage bias conditions defect saturation is not displayed in the QE because of carrier generation in a deeper region of the cell after crossing unabsorbed photons front region.

Index Terms—Band offset, silicon heterojunction (SHJ) solar cells, S-shape, quantum efficiency (QE), voltage and light bias.

I. INTRODUCTION

SILICON heterojunction (SHJ) opens the possibility of using various semiconducting materials as charge selective contacts for solar cells application [1], [2]. With the thin hydrogenated amorphous silicon (a-Si:H) on the crystalline silicon (c-Si) wafer, one can have minimal discontinuities in the bulk properties than the totally different materials as charge selective contacts (emitters), which already demonstrated record conversion efficiency of 26.3% on large area by Kaneka Corporation

Manuscript received February 2, 2018; accepted March 28, 2018. This work was supported in part by the Department of Science and Technology, India, under Clean Energy Research Initiative Grant RP03240 for establishing silicon heterojunction solar cell test facilities and in part by the University Grant Commission (UGC), India. (Corresponding author: Vamsi Krishna Komarala.)

The authors are with the Center for Energy Studies, Indian Institute of Technology Delhi, New Delhi 110016, India (e-mail: sapnamudgal89@gmail.com; spsinghin@gmail.com; vamsi@ces.iitd.ac.in).

Color versions of one or more of the figures in this paper are available online at <http://ieeexplore.ieee.org>.

Digital Object Identifier 10.1109/JPHOTOV.2018.2821839

[3]. The SHJ cell's (Ag/TCO/a-Si:H(p+)/a-Si:H(i)/c-Si(n)/a-Si:H(i)/a-Si:H(n+)/TCO/Ag) microscopic current transport is under intense investigation, [4]–[7] apart from the passivation studies of the c-Si surface for the better device performance [1], [8], [9]. Because of the complexity involved in device structure with different thin layers and their heterointerfaces, one can still consider for using various characterization techniques to understand the current transport mechanism better. The SHJ devices usually suffer from low voltage and poor fill factors (FFs) with S-shape in light current density–voltage (J–V) characteristics because of charge carrier transport issues, such as barrier for charge collection, tunneling through band spike/interface states, multistep tunneling in a-Si:H layers, and recombination via a-Si:H gap states/interface states [4], instead of simple charge carrier diffusion (in neutral bulk) and recombination (in space charge region) in case of homojunction-based silicon solar cells.

From the literature, it can be foretold that the S-shape in the SHJ cells may arise by two types of hindrances in charge carrier collection: 1) Schottky contact (injection barrier) at the transparent conducting oxide (TCO)/a-Si:H interface either in front or back side of the cell because of reverse junction formation [10], and 2) charge carrier accumulation (extraction barrier) at the a-Si:H/c-Si interface because of band offsets and discontinuous bulk/electronic properties [4]. In reality, the band offset at the p-n junction of the SHJ can behave like both as an injection and extraction barrier simultaneously depending on how it blocks the flow of charge carriers from either side of a junction. The J–V measurements alone are not enough to distinguish S-shape from either because of the Schottky contact at TCO/a-Si:H interface or because of band offsets at the a-Si:H/c-Si interface of the SHJ cell [4], [5], [11]. Recently, Das *et al.* [4] adopted the Suns- V_{oc} and quantum efficiency (QE) measurements, and demonstrated the difference of QE behavior from the Schottky barrier and the band offset present within the SHJ cells. Their study was focused only on the QE change in response because of energy barriers existing at the interfaces for the charge carriers, but the responses from the constituent layers of the device are not included.

QE of a solar cell in short-circuit conditions is frequently used to understand charge carrier collection efficiency at different wavelengths of the incident light spectrum [12]. One

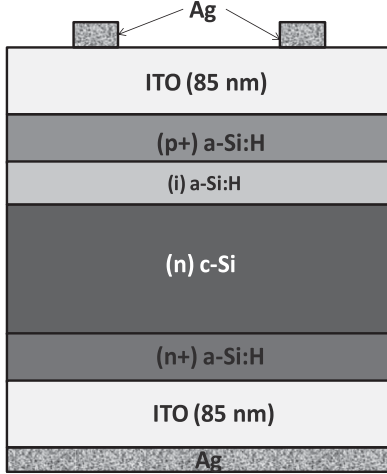


Fig. 1. Schematic of SHJ solar cell used for investigation.

can investigate the device regional issues with QE analysis; by applying voltage bias, the carrier injection can be tuned to understand the carrier tunneling/hopping/thermionic emission mechanism, and with light bias of specific wavelength range (also called photon doping), one can change response from constituent layers to understand the defect states. In this paper, we have selected (Ag/TCO/a-Si:H(p+)/a-Si:H(i)/c-Si(n)/a-Si:H(n+)/TCO/Ag) SHJ solar cell having S-shaped characteristics in its light J-V curve. We try to look into microscopic transport mechanism because of active defect states at the interface and in a-Si:H layers by QE analysis under different light and voltage bias conditions. We made an attempt to identify the regions within the cell behind the poor FF and the reduction of device performance parameters; furthermore, we could correlate the loss of QE because of parasitic absorption loss in the a-Si:H layers.

II. EXPERIMENTAL DETAILS

A. Fabrication of Heterojunction Solar Cell

The schematic of an SHJ cell has been shown in Fig. 1. The cell is fabricated on an n-type monocrystalline Czochralski silicon wafer as a base material having (100) orientation, 180–200 μm thickness and a nontextured surface. Initially, the silicon wafer was treated in an alkaline solution for saw damage removal of about 10- μm -thick layer of silicon material on each side of the wafer. Then, the wafers are given standard Radio Corporation of America cleaning treatment. A brief dip in hydrofluoric acid ($\sim 1\%$) has been given before loading into the plasma-enhanced chemical vapor deposition (PECVD) system. Intrinsic and doped amorphous silicon layers are deposited by RF (13.56 MHz) PECVD. Initially, front side i and p hydrogenated amorphous silicon layers and after that backside n+ hydrogenated amorphous silicon layers are deposited. The thicknesses of (p+)a-Si:H, (i)a-Si:H and (n+)a-Si:H films are ~ 10 , ~ 10 , and ~ 20 nm, respectively. For this solar cell, only the front side is passivated with intrinsic a-Si:H, and the rear side of c-Si n+-a-Si:H is directly deposited on the c-Si wafer to provide back surface field contact. Indium tin oxide (ITO) of ~ 85 nm thickness is deposited on both sides

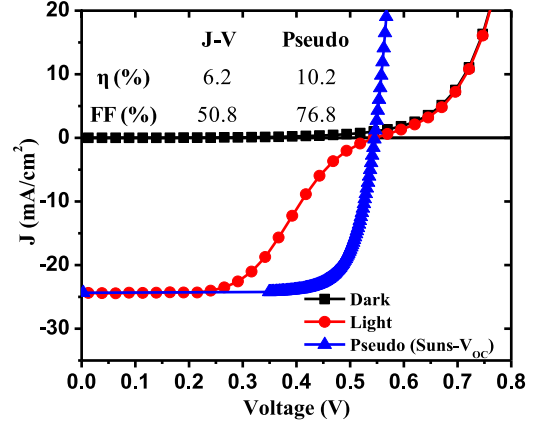


Fig. 2. Current J-V characteristics of the SHJ solar cell under dark and light measurement conditions, along with the pseudo J-V graph from Suns- V_{oc} measurement.

of the cell by pulsed dc magnetron sputtering in plasma of oxygen ($\sim 1\%$) argon mixture. Front and back metallization were done by screen printing and curing of low-temperature silver (Ag) paste. More details of fabrication method are presented by Chandril *et al.* [13].

B. Device Characterization

After fabrication of large area 5" pseudosquare SHJ solar cell, we have selected a small area of 5.5 cm^2 for the electrical measurements. In order to see the series resistance-free electrical performance of this device, the Suns- V_{oc} measurement has been done using the Sinton WCT-120 instrument. The current J-V characteristics were performed under standard test conditions (room temperature and AM1.5G spectrum) by the Oriel class AAA solar simulator (Newport, USA) using Keithley 2440 as a source meter. The intensity of AM1.5G spectrum was varied for different sun's illumination with the help of neutral density filters.

The external quantum efficiency (EQE) and total reflectance of the solar cell were measured at room temperature using the SpeQuest QE measurement system from ReRa solutions, The Netherlands. The internal quantum efficiency (IQE) was estimated from the EQE and total reflectance data. To modulate the incident light spectrum, the chopping frequency of the optical chopper has been kept at 183 Hz for all EQE measurements. The incident chopped monochromatic beam spot was of ~ 3 -mm diameter. This system has provision for the voltage bias and light bias with different wavelengths. Inbuilt dc voltage supply was used for forward and reverse biasing of the SHJ cell. The EQE is recorded without and with (blue, infrared, and white) light bias conditions at different voltages in order to investigate an S-shaped J-V graph to understand the charge carrier transport barrier.

III. RESULTS AND DISCUSSION

A. Current-Voltage Characteristics

The graphs of dark and light J-V characteristics are shown in Fig. 2. Within the fourth quadrant of light J-V, the carrier

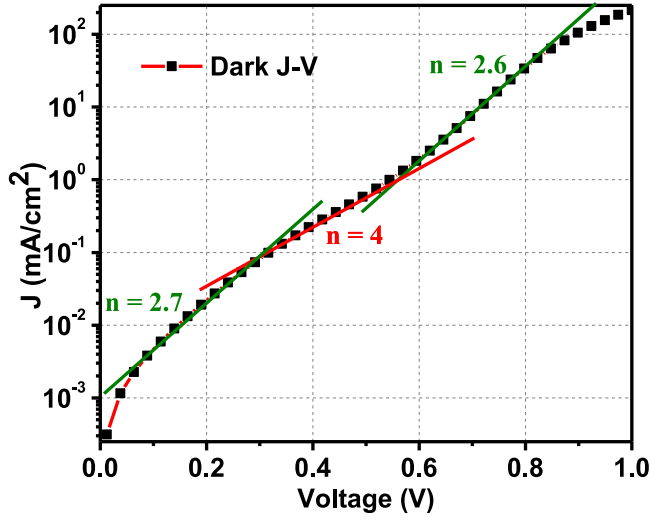


Fig. 3. Semilogarithmic dark J-V curve of the SHJ solar cell along with ideality factors for three different linear regions after curve fitting.

collection is severely affected for $V > 0.3$ V and the concave shape is observed, instead of the convex shape (“J” shape) usually observed for conventional homojunction silicon solar cell. This concave shape has been referred as S-shaped characteristics in the literature. Such S-shape can severely reduce the FF and, thus, degrade cell’s performance. The Suns- V_{oc} measurement (see Fig. 2) has also been done for this solar cell using the Sinton Suns- V_{oc} setup to neglect the series resistance effect on the J-V characteristics. Calibration has been done using $J_{sc} = 24.3$ mA/cm² as observed from the light J-V characteristics. In the pseudo J-V curve, the FF is improved from 50.8% to 76.8%. In order to understand the origin of this S-shape responsible for such a high FF loss in an actual J-V curve, the dark J-V is also recorded, and the ideality factors are estimated for different linear regions of the J-V graph.

The semilogarithmic J-V ($\ln J$ -V) graph in the dark for the SHJ solar cell is presented in Fig. 3, wherein three linear regions are observed. A high value of ideality factors (>2) is observed from the slopes of the linear regions of the $\ln J$ -V plots in all three linear regions, which are difficult to explain with the help of charge transport mechanisms based on the conventional p-n or p-i-n junction. Three linear regions in the graph with high ideality factors indicate that the device with large defect densities, which are assisting the loss of charge carriers by recombination during transport through multiple steps hopping/tunneling as explained by Matsuura *et al.* [6]. Chavali *et al.* also reported ideality factors $n \gg 2$ because of the presence of defect-assisted tunneling in these particular voltage ranges [14].

To find out the possible transport barrier responsible for the S-shape in light J-V graph, the J-V characteristics are recorded at different illumination intensities and are shown in Fig. 4(a) along with their normalized plots of photocurrent ($J_{ph} = J - J_D$, where J is the total current and J_D is the dark current) with J_{sc} of the cell shown in Fig. 4(b). The curvature of S-shape is found diminishing for the lower excitation light intensities, which indicates that the junction field inside the device at lower light intensities is sufficient to overcome the carrier blocking

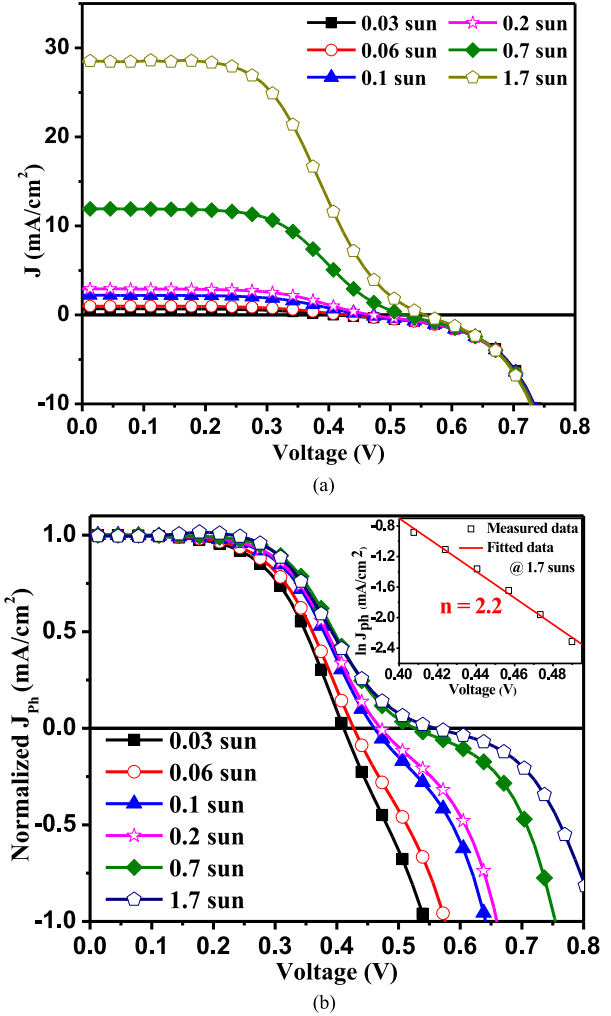
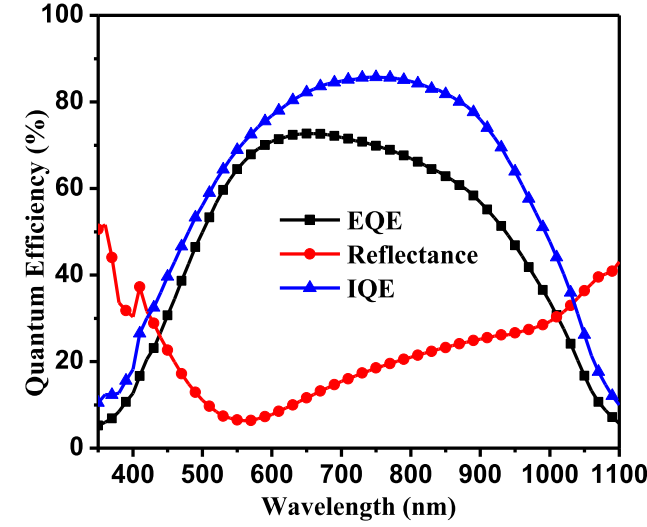


Fig. 4. (a) Light intensity dependent J-V graphs and (b) normalized photo-generated current density ($J_{ph} = J - J_D$, where J is the total current and J_D is the dark current) with J_{sc} of SHJ solar cell; inset of (b) shows the semilog plot between photocurrent and voltage at 1.7 suns.

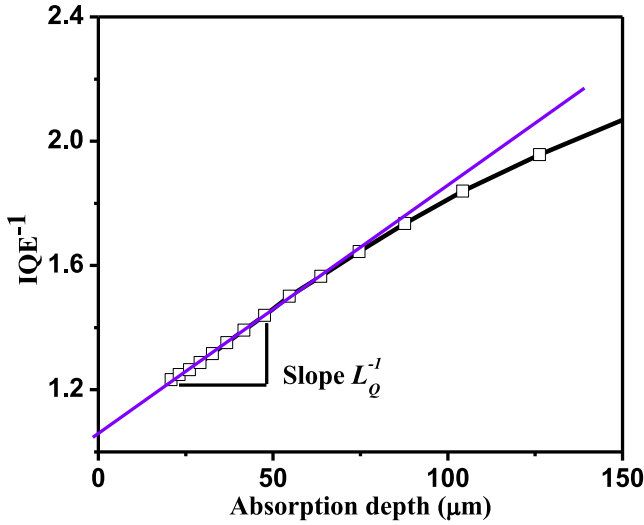
barrier for voltages below the open circuit. At lower intensities, the quasi-Fermi level splitting is less, so, less reduction in the junction field is created, leaving sufficient junction field to overcome the charge carrier barrier [5]. However, this can also create lower V_{oc} in the device since the photocurrent is not blocked; there will not be any S-shape in the J-V plot. At higher intensities, the S-shape is more visible because of the weakening of the junction field near V_{oc} under higher light bias conditions arising because of the large quasi-Fermi level splitting. To verify the loss of charge carriers; the $\ln J_{ph}$ versus voltage graph of 1.7 sun illumination is also plotted [see inset of Fig. 4(b)], the diode quality factor is 2.2 in the S-shaped regime, which shows that the loss of charge carriers is because of recombination in the junction interface region.

B. Charge Collection Response From Quantum Efficiency Analysis

The spectral dependence of the charge carrier collection is measured to identify the regions of problems in the device.



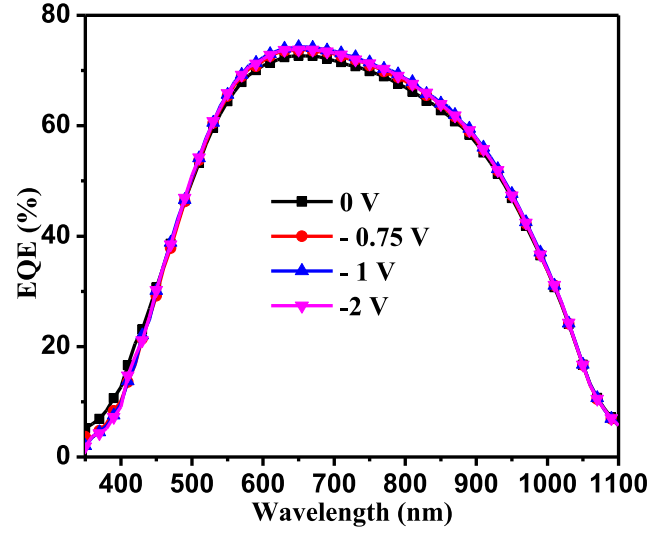
(a)



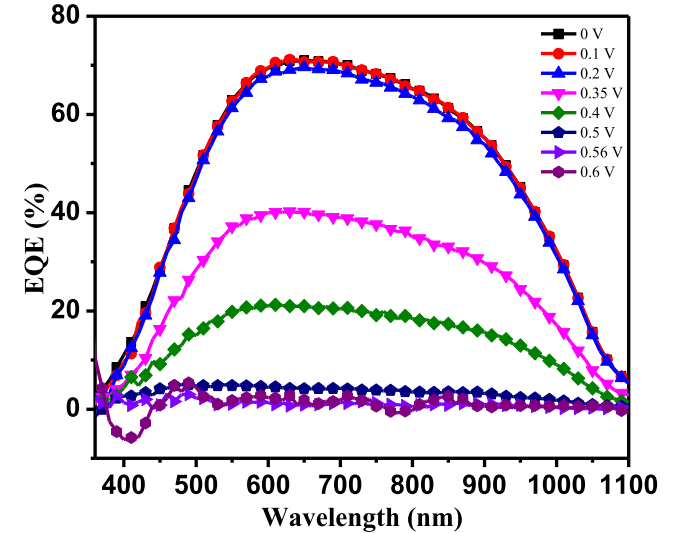
(b)

Fig. 5. (a) Measured EQE, reflectance, and estimated IQE spectra of the SHJ cell and (b) graph between IQE^{-1} and absorption depth (α^{-1}) along with the curve fitted line.

Initially, cell's EQE is measured at short-circuit conditions without voltage and light bias, which is shown in Fig. 5(a). Since the device is fabricated on a nontextured wafer, IQE is also calculated after correction for the reflectance of the cell. The reflectance loss is quite high in the longer wavelength region than the shorter wavelength region. To check the quality of silicon surface passivation, the IQE response with absorption depth is also presented in Fig. 5(b), which shows a linear region for thickness lesser than the base wafer. At lower absorption depth than the thickness of the cell, the slope is defined as an effective QE diffusion length (L_Q), which can be measured under the carrier injection regime [15]. The L_Q value of $\sim 120 \mu\text{m}$ is obtained after fitting the curve, which is lower than the thickness of the wafer. The diffusion length of $\sim 125 \mu\text{m}$ is also evaluated (using the relation $L = \sqrt{D\tau}$, where D is the diffusion coefficient, and τ is the minority carrier lifetime) from the effective lifetime value obtained from the Suns- V_{oc} measurement.



(a)



(b)

Fig. 6. EQE of the SHJ cell at (a) reverse- and (b) forward-bias voltages without light bias.

The values of diffusion length from the IQE and lifetime measurements are nearly same, which indirectly reflects the loss of photo-generated charge carriers because of the higher recombination at the interfaces. The QE of the cell is further investigated under voltage and light bias conditions; therefore, one can have an idea on the carrier injection level dependent recombination processes for providing the better explanation to the S-shaped light J-V characteristics.

First, the QE is measured at the reverse-bias condition by applying -0.75 to -2 V [see Fig. 6(a)], in order to see whether the junction field is sufficient enough at zero bias condition or not. Since there is no significant improvement in the EQE at reverse bias in comparison with the zero-voltage bias, it can be assumed that the field at zero bias is sufficient enough to separate the photo-generated charge carriers. Then, the device QE is measured by forward biasing [see Fig. 6(b)], which is quite revealing. The EQE does not show much variation till the starting

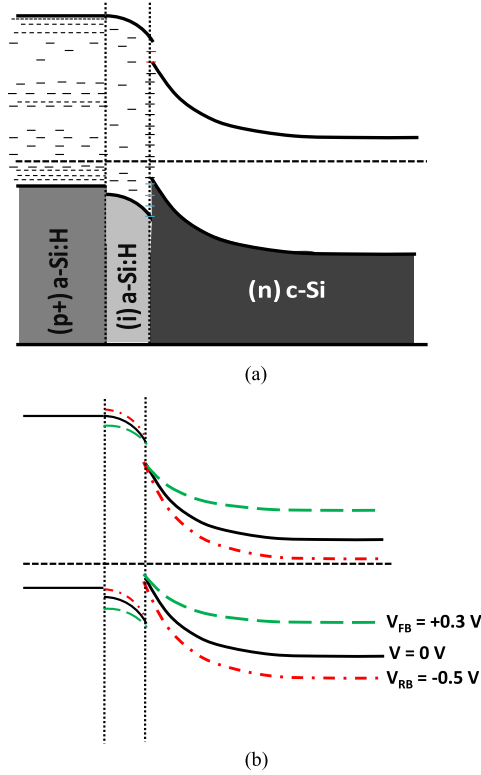


Fig. 7. Energy band diagrams (a) under thermodynamic equilibrium with electronic defect states in the bandgap of a-Si layers and (b) electronic band diagram of (front side) a-Si:H(p+)/a-Si:H(i)/c-Si(n) heterojunction without and with forward-/reverse-bias voltage.

point of S-shape (~ 0.3 V); a further increase in the forward-bias voltage has shown a gradual reduction of the EQE in the entire wavelength region. Since the dark I - V characteristics do not have the S-shaped feature and the onset of the significant dark current flow takes place at biases higher than the V_{oc} of the cell, the photocurrent loss can be attributed to the difficulty in the charge collection, which may be because of the hindrance created by some kind of barrier. In addition, the cell bias voltage beyond V_{oc} , negative EQE around 400 nm, is observed. As photocurrent has been overtaken by the dark current after V_{oc} , the current generated in the regions of a-Si layers flows in the forward direction under this bias condition. This may also be an indication of contribution from the photoconductivity of amorphous silicon layers [16], wherein intrinsic amorphous silicon is quite photoconductive.

Fig. 7 shows the device energy band diagram under the thermal equilibrium condition with the band offset at the a-Si:H(i)/c-Si heterointerface and electronic defect states in the bandgap of a-Si layers, and an energy band diagram with different voltage bias conditions. The charge carriers move hopping through a large number of traps and recombination centers present in the bandgap of intrinsic and p-type a-Si:H layers under application of voltage bias. Initially, the minority charge carriers (holes) generated by light in the c-Si have to surmount the energy barrier at the junction region to reach the hole accepting a-Si:H(p+) layer. At the zero-voltage bias condition, the electrostatic field

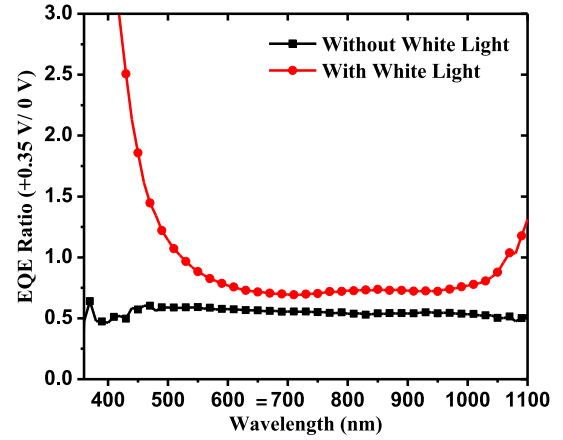


Fig. 8. SHJ cell's EQE ratio of +0.35 to 0 V without and with white light bias (0.3 suns) conditions.

of the junction is higher and sufficient to push the holes over the band offset for the collection at the front contact. Under the reverse-bias condition [see Fig. 6(a)], junction field further increases and the holes do not have a barrier in crossing the valence band offset. On the other hand with the forward-bias voltage, the junction field started collapsing, and the barrier [see Fig. 7(b)] stands tall enough to hinder the flow of holes to the hole-accepting a-Si:H(p) layer [see Fig. 6(b)]. Therefore, the charge carrier collection efficiency is reduced with the +0.35 V voltage bias and above.

Conventional silicon solar cells do not have issues with voltage biasing in the EQE [17], since charge carrier collection is mainly because of the diffusion and not by the drift. In the case of the a-Si/c-Si SHJ solar cell, a large number of defects are expected in the junction region because of the defect-prone a-Si layers and their interfaces. To investigate this, the EQE of the device is measured at +0.35 V (S-shaped starting voltage) bias along with the blue (~ 455 nm), red (>810 nm), and white light bias (0.3 suns) conditions. Fig. 8 shows the EQE ratio of +0.35 V to 0 V without and with white light bias conditions. The EQE of the cell at 0.35 V bias is almost half of the EQE at 0-V bias condition, and is also wavelength independent without white light bias conditions; however, with white light bias, cell's QE is enhanced for all the wavelengths. Our results followed the trend of QE characteristics change observed by Das *et al.* [4]; the carrier transport hindrance is due to the band offset at the a-Si/c-Si interface rather than the Schottky barrier present at the ITO/(p)a-Si:H interface. However, in our case under the white light bias condition, the EQE ratio is not wavelength independent, and it is larger in blue and red wavelength regions that stipulate the highly defective a-Si layers and the a-Si/c-Si interfaces of the device. Since the amount of enhancement under the white light is much higher in the violet and blue regions than the red wavelength region, the front region (emitter) can be severely defective.

Fig. 9(a) shows the EQE spectra of SHJ cell at +0.35 V and with different light bias conditions (white, infrared, and blue), for reference EQE spectrum of the cell without light, and the voltage bias is also presented. The EQE response of the cell at

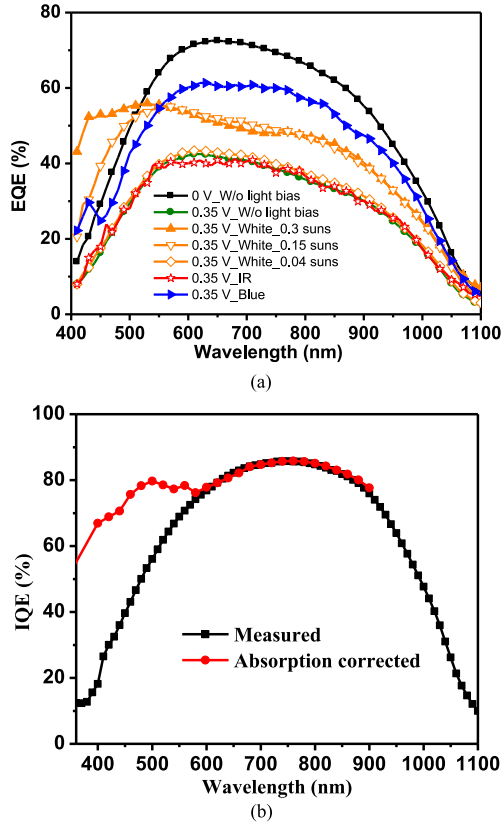


Fig. 9. (a) EQE spectra of an SHJ cell at +0.35 V and with different light bias conditions and (b) IQE without light and voltage biasing along with the absorption corrected for amorphous silicon layers in the IQE as a function of wavelength.

+0.35 V and IR light bias has shown no modification in comparison with only the +0.35 V bias condition, which indicates that the response of the device from a deeper region is not light dependent, and the defect saturation effect is not displayed. The EQE of the cell under +0.35 V and the blue light bias condition is improved uniformly throughout the wavelength range because of the reduction in charge carrier recombination, and mainly because of the defect saturation in the a-Si:H layers at the junction region with an additional photocarrier generation. The EQE experiments also performed with different white light intensity along with the +0.35 V bias. The EQE of the cell under +0.35 V and 0.3 suns white light bias improved the charge collection efficiency in all wavelength regions differently and even crossed the response of unbiased cell's EQE at shorter wavelengths, which means that the interface defects and trap states in the a-Si:H layers responded differently. If the intrinsic a-Si:H layer is defective, then the possibility of multistep tunneling is highly probable for both types of charge carriers, and this will increase the chance of undesirable recombination of electrons and holes that can reduce the V_{oc} of the device significantly [11]. The EQE enhancement in the short wavelength region under 0.3 suns white light bias is attributed to the enhancement in photoconductivity (optical injection based modulation of conductivity) of the intrinsic a-Si:H buffer layer, and the reduction in geminate recombination because of the defect saturation at the light facing interfaces. The a-Si:H layers have a large num-

ber of traps and recombination centers generated because of dangling and strained bonds; the excess carriers generated under voltage and light bias conditions can enhance hole tunneling across a large barrier in the front emitter side. The probability of charge carrier recombination is dependent on the availability of the free charge carriers and the number of active defect states. The EQE response in short wavelength (400 to 500 nm) region reduced with 0.15 suns in comparison with 0.3 suns white light bias because of the reduction in the defect saturation in the a-Si:H layers. With 0.04 suns white light bias intensity, the EQE response reduced and almost overlapped with the EQE spectrum at 0.35 V bias (without light bias) because of unaffected defect states in the a-Si:H layers. The EQE modification with fixed bias +0.35 V and white light intensity variation in Fig. 9(b) correlates with the intensity-dependent light J-V characteristics (see Fig. 4).

In this study, the thicker a-Si layers are used to avoid shorting of the device; the loss because of absorption is estimated by taking absorption coefficient values for a-Si layers from the AMPS 1 D software database [18], and the absorption corrected IQE is presented in Fig. 9(b). It can be seen that there is a significant improvement in the blue region after parasitic absorption correction in the a-Si:H layers. The profile of absorption corrected EQE of the cell in the blue region [see Fig. 9(b)] is similar to the EQE under +0.35 V and the white light bias condition [see Fig. 9(a)]. It indicates that cell's EQE improvement in the blue region under the bias condition is due to current collected from the carriers generated by absorption of radiation in the intrinsic a-Si:H layer. Much thicker i- and p-a-Si:H layers can also have significant impact on the electrostatics of cell's junction, and can further introduce some modification in the junction field or depletion width with voltage and light bias conditions. The thicker defective nature of a-Si:H layers is also supported by the fact that the dark current has a higher ideality factor.

IV. CONCLUSION

SHJ solar cell's nonideal S-shaped characteristics under light are analyzed by the J-V and QE measurements. The J-V characteristics under different illumination intensities revealed that they are collection dependent. The EQE under voltage and different light bias conditions revealed that the cell has defective amorphous layers and a large barrier because of the band offset at the front-side heterointerface of a-Si and c-Si, which hinder photocarrier collection after the carrier generation. The QE can be a powerful characterization technique with different voltage and light bias to understand the photoactive layers' defects and the p-n junction interface defects effectively to region out the problems responsible for S-shape in light I -V characteristics of a SHJ and charge selective contacts based silicon and thin film cells that affects the device energy conversion efficiency.

ACKNOWLEDGMENT

The authors wish to thank amorphous silicon R&D plant of Bharat Heavy Electrical Limited, India for the fabrication of devices.

REFERENCES

- [1] C. Battaglia *et al.*, “Silicon heterojunction solar cell with passivated hole selective MoO_x contact,” *Appl. Phys. Lett.*, vol. 104, no. 11, Mar. 2014, Art. no. 113902.
- [2] M. Mews, A. Lemaire, and L. Korte, “Sputtered tungsten oxide as hole contact for silicon heterojunction solar cells,” *IEEE J. Photovolt.*, vol. 7, no. 5, pp. 1209–1215, Sep. 2017.
- [3] Y. Kunta *et al.*, “Silicon heterojunction solar cell with interdigitated back contacts for a photoconversion efficiency over 26%,” *Nature Energy*, vol. 2, no. 5, Mar. 2017, Art. no. 17032.
- [4] U. Das, S. Hegedus, L. Zhang, and J. Appel, “Investigation of hetero-interface and junction properties in silicon heterojunction solar cells,” in *Proc. 35th IEEE Photovolt. Spec. Conf.*, 2010, pp. 001358–001362.
- [5] R. V. K. Chavali *et al.*, “A generalized theory explains anomalous Suns-V_{oc} response of Si heterojunction solar cells,” *IEEE J. Photovolt.*, vol. 7, no. 1, pp. 169–176, Jan. 2016.
- [6] K. Matsuura, H. Okuno, T. Okushi, and H. Tanaka, “Electrical properties of n-amorphous/p-crystalline silicon heterojunctions,” *J. Appl. Phys.*, vol. 55, pp. 1012–1019, 1984.
- [7] W. van Sark, L. Korte, and F. Roca, *Physics and Technology of Amorphous-Crystalline Heterostructure Silicon Solar Cells*. Berlin, Germany: Springer, 2012, pp. 1–12.
- [8] K. Nakada, S. Miyajima, and M. Konagai, “Amorphous silicon oxide passivation films for silicon heterojunction solar cells studied by hydrogen evolution,” *Jpn. J. Appl. Phys.*, vol. 53, no. 4S, Jan. 2014, Art. no. 04ER13.
- [9] M. Kondo, S. De Wolf, and H. Fujiwara, “Understanding of passivation mechanism in heterojunction c-Si solar cells,” *MRS Online Proc. Library Arch.*, vol. 1066, Jan. 2008, Art. no. 1066–A03-1.
- [10] M. Ghannam, Y. Abdulraheem, and G. Shehadeh, “Interpretation of the degradation of silicon HIT solar cells due to inadequate front contact TCO work function,” *Solar Energy Mater. Solar Cells*, vol. 145, pp. 423–431, Feb. 2016.
- [11] A. Froitzheim, R. Stangl, L. Elstner, M. Kriegel, and W. Fuhs, “AFORS-HET: A computer-program for the simulation of heterojunction solar cells to be distributed for public use,” in *Proc. 3rd World Conf. Photovolt. Energy Convers.*, vol. 1, 2003, pp. 279–282.
- [12] D. Lan and M. A. Green, “Extended spectral response analysis of conventional and front surface field solar cells,” *Solar Energy Mater. Solar Cells*, vol. 134, pp. 346–350, Mar. 2015.
- [13] S. Chandril, M. Pathak, V. Bhardwaj, A. Sharan, and N. Chahar, “Dependence of silicon heterojunction solar cell performance on surface preparation, deposition conditions, chemical treatment and annealing,” *Int. J. Renewable Energy. Res.*, vol. 3, no. 4, pp. 1–4, 2013.
- [14] R. V. K. Chavali, J. R. Wilcox, B. Ray, J. L. Gray, and M. A. Alam, “Correlated nonideal effects of dark and light I-V characteristics in a-Si/c-Si heterojunction solar cells,” *IEEE J. Photovolt.*, vol. 4, no. 3, pp. 763–771, May 2014.
- [15] R. Brendel, *Thin-Film Crystalline Silicon Solar Cells: Physics and Technology*. New York, NY, USA: Wiley, 2005, pp. 241–250.
- [16] Z. Cheng *et al.*, “Working quantum efficiency of CdTe solar cell,” in *Proc. 35th IEEE Photovolt. Spec. Conf.*, 2010, pp. 001912–001914.
- [17] X. X. Liu and J. R. Sites, “Solar-cell collection efficiency and its variation with voltage,” *J. Appl. Phys.*, vol. 75, no. 1, pp. 577–581, Jan. 1994.
- [18] “Analysis of microelectronic and photonic structures,” [Online]. Available: <http://www.ampsmodeling.org/materials/naSiopt.htm>. Accessed on: Sep. 18, 2017.



Sapna Mudgal received the M.Sc. degree in physics from Dr. Bhimrao Ambedkar University, Agra, India, in 2010, and the M.Tech. degree in energy studies, in 2014, from the Indian Institute of Technology Delhi, New Delhi, India, where she is currently working toward the Ph.D. degree in investigation of silicon heterojunction solar cells.

Her current research focuses on understanding electronic transport in silicon heterojunction solar cells using different characterizations, data fitting, and simulation of devices.



Sonpal Singh received the M.Tech. degree in solid state materials and the Ph.D. degree in indium tin oxide/silicon heterojunction solar cells from the Indian Institute of Technology Delhi, New Delhi, India, in 1980 and 1986, respectively.

He is currently a Consultant in a project for the fabrication and characterization of heterojunction cells. From 1986 to 1989, he was a Scientist in IIT Delhi on a project for the deposition and characterization of silicon nitride and silicon oxide films by plasma and photo CVD for IC fabrication. From 1989 to 2016,

he was with the Amorphous Silicon Solar Cell Plant, Bharat Heavy Electricals Limited, Haridwar, India, for the development of amorphous silicon solar cells/modules and heterojunction cells based on amorphous silicon–crystalline silicon interfaces. His research interest includes the study of passivation mechanism of silicon surface by solution and plasma treatments, fabrication of heterojunction devices, and characterizations of layers and devices.



Vamsi Krishna Komarala was born in Muddanur, India, in 1974. He received the B.Sc. and M.Sc. degrees in physics from Sri Venkateswara University, Tirupati, India, in 1994 and 1996, respectively, the M.Tech. in energy science and technology from Jadavpur University, Kolkata, India, in 1999, and the Ph.D. degree from the Indian Institute of Technology Delhi, New Delhi, India, in 2004.

From 2004 to 2007, he was a Postdoctoral Fellow with the Trinity College Dublin, and from 2007 to 2010, a Research Associate with the University of Arkansas, Fayetteville, AR, USA. Since 2010, he has been associated with the Center for Energy Studies, Indian Institute of Technology Delhi, initially as an Assistant Professor from 2010 to 2014, and as an Associate Professor since 2014. He has contributed more than 50 research papers in international journals. His research interests include plasmonics for solar cells application and heterojunction solar cells. His teaching focus is on nonconventional sources of energy and direct energy conversion methods.